

Available online at www.sciencedirect.com**SciVerse ScienceDirect**

Procedia Environmental Sciences 12 (2012) 298 – 304

Procedia

Environmental Sciences

2011 International Conference on Environmental Science and Engineering
(ICESE 2011)

Influence of Particle Initial Temperature on High Velocity Impact Process in Cold Spraying

Yue Li, Xiao-fang Wang, Shuo Yin, Sheng-li Xu

*School of Energy and Power Engineering Dalian University of Technology Dalian, China
ly72141@gmail.com, yinshuo0511@yahoo.cn*

Abstract

In this study, coupled thermal-mechanical analysis of particle impact behavior in cold spraying was conducted for Cu by using ABAQUS program. Some important aspects on particle initial temperature in cold spraying were examined. The results show that initial temperature of particle takes an important role in 3D simulated results. As the initial temperature rising, compression ratio of the particle increases gradually, critical velocity decreases, but depth of the pit charges little. Furthermore, particle initial temperature has some influence on interface temperature rising and the maximum temperature did not occur at the centre point of initial impact.

© 2011 Published by Elsevier B.V. Selection and/or peer-review under responsibility of National University of Singapore.
Open access under [CC BY-NC-ND license](http://creativecommons.org/licenses/by-nc-nd/3.0/).

Keywords: Cold spraying; Numerical simulation; Initial temperature; Coupled thermal-mechanical analysis

1. Introduction

Cold spraying, also called cold gas-dynamic spray, re-presents a radical difference from conventional thermal spray methods. Compared with the conventional thermal spray, cold spray particles (typically $<50\mu\text{m}$) are accelerated to a high velocity (ranging from 300 to 1200m/s) by the super-sonic gas flow which is generated in the convergent-divergent de Laval nozzle. A coating is formed through the intensive plastic deformation of particles at a temperature well below the melting point of spray material. Additionally, cold spray has many advantages, such as the wider choices of metals and alloys as coating materials, the capability of oxygen-free coating and high deposition efficiency.

During the past decade, some investigations on impact process and particle deformation behavior in cold spraying have been conducted though both experimental and numerical methods by different researchers. Owing to the extremely short duration of the impact process, it is difficult to observe the

whole particle deformation by experiment. Only the deformed particle can be observed experimentally. Therefore, numerical methods are always employed to study the particle deformation process[1-3].

In this study, through numerical simulation by ABAQUS, with the Dynamic-Temp-Disp-Explicit procedure, the role of the particle initial temperature in cold spraying is analysed.

2. Numerical modeling

2.1 Numerical method

The impact behavior of the Cu particle upon the Cu substrate was modeled by using an explicit FEA program ABAQUS. Lagrange formulations were employed in solution based on mass, momentum and energy conservation equations. Simulations were solved in conjunction with appropriate boundary conditions and material constitutive model. Compared to the high inertial force from the high speed carrying flow, all body forces, such as gravity, were neglected. Three-dimensional models were used to simulate the particle deformation behavior. For reducing the element number and shortening the calculation time, the three-dimensional models were simplified as a 1/2 symmetric model, the radius and height of the substrate were taken to be 4 and 6 times larger than the particle radius as shown in Fig. 1. All the contact processes were implemented by using the surface to surface penalty formulation available in ABAQUS. The meshing was conducted using reducing integral Hex-ahedral elements(C3D8RT). A fixed boundary condition was applied to the bottom plane and a free boundary condition for the others.

The initial velocity of particle is fixed at a moderate value of 500m/s because Lagrange algorithm on grid quality request is high, if particle velocity is excessive, serious distortion of grids occurs and the computer program is terminated. But with the velocity of 500m/s, the simulations work well in most cases. In addition, the impacting velocity of 500m/s is greater than the critical velocity of copper particle and copper substrate adhesion[5].

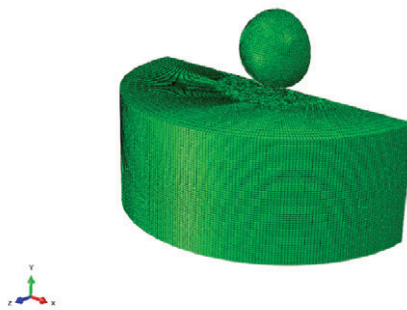


Figure 1. Geometry model and meshing of particle and substrate

2.2 Material model

For particles and substrates, the material deformation was described by the Johnson and Cook plasticity model, which accounts for strain hardening, strain rate hardening and thermal softening effects. The stresses were expressed according to the Von Mises plasticity model. The yield stress (σ) of this material is expressed as follows[3,4]:

$$\sigma = (A + B\varepsilon_p^n) (1 + C \ln(\varepsilon^*)) (1 - (T^*)^m) \tag{1}$$

where A, B, n, C, m are material-related constants dependent on materials. ε_p is the effective plastic strain (PEEQ). ε^* is the effective plastic strain rate normalized with respect to a reference strain rate. T^* is a homologous temperature defined as the following:

$$T^* = \frac{T - T_0}{T_m - T_0} \tag{2}$$

Where T_m is the melting point and T_0 is the reference or transition temperature.

The Johnson and Cook dynamic failure model was used which accounts for the effects of hydrostatic pressure, strain rate and temperature. The Johnson and Cook dynamic failure model is based on the value of the equivalent plastic strain at element integration points, where failure is assumed to occur when the damage parameter exceed 1. The damage parameter, ω is defined as

$$\omega = \sum \left(\frac{\Delta \varepsilon_p}{\varepsilon_{pf}} \right) \tag{3}$$

where $\Delta \varepsilon_p$ is an increment of the equivalent plastic strain, ε_{pf} is the strain at failure, and the summation is performed over all increments in the analysis. The strain at failure is assumed to be dependent on a nondimensional plastic strain rate ε^* ; a dimensionless pressure-deviatoric stress ratio, p/q (where p is the pressure stress and q is the Mises stress); and the nondimensional temperature, T^* , defined earlier in the Johnson and Cook plasticity model. The dependencies are assumed to be separable and are of the form :

$$\varepsilon_{pf} = [d_1 + d_2 \exp(d_3 \frac{p}{q})] [1 + d_4 \ln(\varepsilon^*)] (1 - (T^*)^m) \tag{4}$$

Where $d_1 - d_5$ are failure parameters measured at or below the transition temperature, T_0 . When this failure criterion is met, the deviatoric stress components are set to zero and remain zero for the rest of the analysis.

Table 1 Properties of ofhc copper used in simulations

Parameter	Cu
Density, kg/m ³	8960
Thermal conductivity, W/(mK)	386
Specific heat, J/kgK	383
Melting point, K	1356
Elastic modulus,GPa	124
Poisson's ratio	0.34
JC plasticity: A,MPa,B,MPa,n,C,m	90, 292, 0.31, 0.025, 1.09
JC damage:d ₁ ,d ₂ ,d ₃ ,d ₄ ,d ₅	0.54, 4.89, -3.03, 0.014, 1.12
Reference temperature,K	298
Reference strain rate,1/s	1

3. results and discussion

Fig.2 shows the typical experimental observation of deformed Cu particle on Cu substrate (a) and the typical 3D simulation results on the deformed Cu particle upon Cu substrate with the distribution of the effective plastic strain of deposited particles after impacting at 500m/s. According to the distribution of effective plastic strain, it is found that the narrow interfacial region has experienced intensive deformation and a crater has been developed in the flat substrate. For 3D simulation, the metal jet at the surround-ing

of the particle is not prominent and extends much weaker than that at the surrounding of the substrate. Most part of particle are submerged within the substrate.

The contours of the deformed particle obtained by 3D model seem to be comparable to the experimental observation that shows the accuracy of the numerical calculation.

Fig.3 shows the distribution of the effective plastic strain of deposited particles after impacting at 500m/s with different particle initial temperature. As can be seen from the figure, with the rising of particle initial temperature, center length of the particle decreased, the degree of flattening increased, the metal jet at the surrounding of the particle was more prominent, however, the range of effective plastic strain changed little. Moreover, the maximum plastic deformation is concentrated at the surrounding of the contact zone rather than at the centre point of initial impact. It is reasoned that the adhesion strength of particle and substrate is low at the centre point of initial impact.

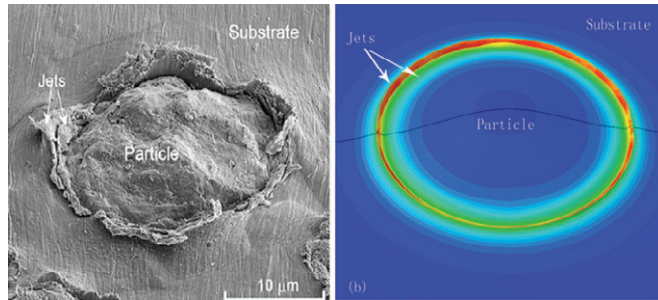


Figure 2. The typical experimental observation (a)[8] and 3D simulation results (b) on the deformed Cu particle upon Cu substrate

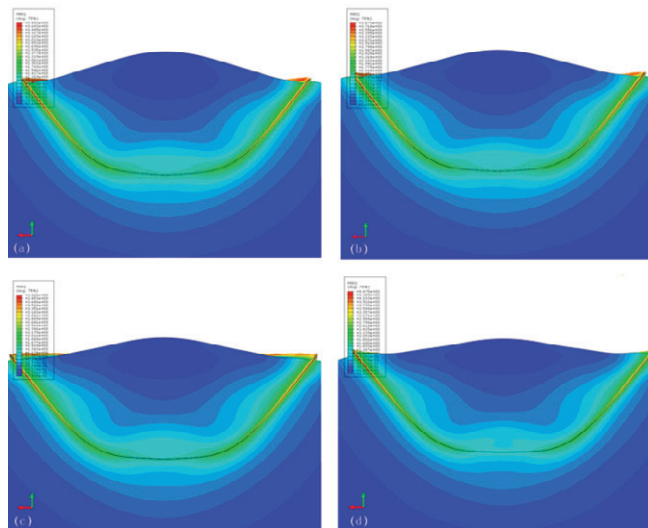


Figure 3. 3D simulation results of effect of particle initial temperature on the particle deformed shape and effective plastic strain

Fig.4 shows the temperature distribution of particle and substrate after impacting. It is can be seen that the maximum temperature is concentrated at the surrounding of the contact zone rather than at the centre point of initial impact. With the rising of particle initial temperature, the maximum temperature increased, but still lower than the melting point of copper, therefore, in the process of collisions, particles and

substrate do not melt, which can be concluded the melting is not the key factor of particle and substrate bonding.

Local plastic strain of contact zone combination with thermal softening effect promoted adiabatic shear instability occurring and resulted in metal jet around the particle and substrate. This is consistent with the conclusion of Grujicic .

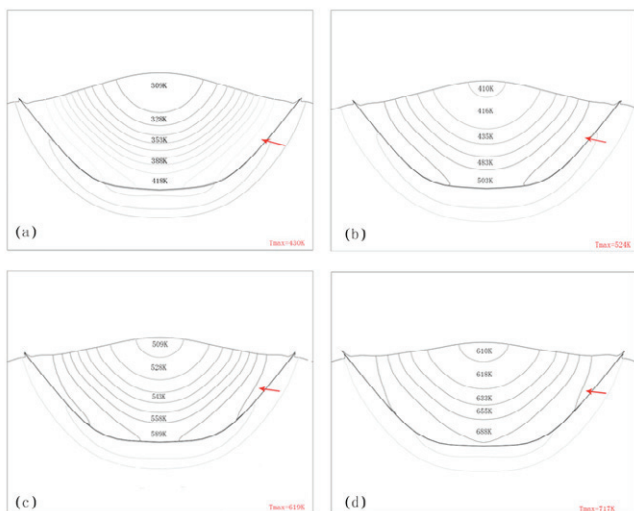


Figure 4. 3D simulation results of the temperature distribution after impacting

Fig.5 shows Variation of contact area with particle initial temperature. The higher of particle initial temperature, the greater of contact area, therefore, higher particle initial temperature is conducive to the bonding of particle and substrate.

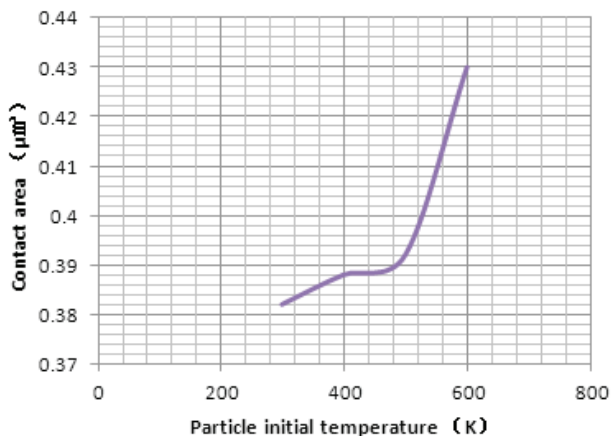


Figure 5. Variation of contact area with particle initial temperature

Fig.6 (a) shows variation of compression ratio with particle initial temperature. It is clear that the compression ratio increases gradually with particle initial temperature. When particle initial temperature

exceeded 498K, the curve of compression ratio has jumped slope. Higher compression ratio indicates more intense deformation of the particle.

Fig.6 (b) shows the temporal development of effective plastic strain under different particle initial temperature .It can be seen that the higher of particle initial temperature, the greater of effective plastic strain. When particle initial temperature exceeded 498K, the maximum effective plastic strain was greatly raised.

In conclusion, higher particle initial temperature is conducive to the bonding of particle and substrate.

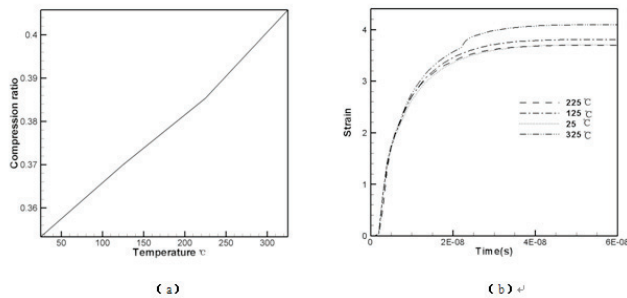


Figure 6. variation of compression ratio with particle initial temperature (a) and the temporal development of effective plastic strain under different particle initial temperature (b)

4. Conclusions

1) The maximum plastic deformation and the maximum temperature are concentrated at the surrounding of the contact zone rather than at the centre point of initial impact. Adhesion strength of particle and substrate is low at the centre point of initial impact.

2) Higher particle initial temperature is conducive to the bonding of particle and substrate.

3) With the rising of particle initial temperature, the maximum temperature increased, but still lower than the melting point of copper, therefore, in the process of collisions, particles and substrate do not melt, which can be concluded the melting is not the key factor of particle and substrate bonding

5. Acknowledgment

The authors would like to acknowledge the financial support by the National Natural Science Foundation of China (No. 50476075).

References

- [1] Shuo Yin Wen-Ya Li Bao-peng Xu, "Numerical Investigation on Effects of Interactions Between Particles on Coating Formation in Cold Spraying," *Journal of Thermal Spray Technology*, 686-vol 18(4) Dec 2009.
- [2] Shuo Yin Xiao-fang Wang, "3D numerical simulation of high velocity impact process in cold spraying," *Explosion and shock waves*, vol 30(5) Sept.2010.
- [3] Wen-Ya Li, Wei Gao, "Some aspects on 3D numerical modeling of high velocity impact of particles in cold spraying by explicit finite element analysis," *Appl. Surf. Sci.* (2009), doi:10.1016/j.apsusc.2009.04.135.
- [4] Wen-Ya Li, Chao Zhang, Chang-Jiu Li, Hanlin Liao. "Modeling Aspects of High Velocity Impact of Particles in Cold Spraying by Explicit Finite Element analysis," *Journal of Thermal Spray Technology*. doi:10.1007/s11666-009-9325-2.2009.05.

- [5] Wen-Ya Li Hanlin Liao, “ On high velocity impact of micro-sized metallic particles in cold spraying,”
doi:10.1016/j.apsusc.2006.05.126.
- [6] M. Grujicic, C.-L. Zhao, W.S. DeRosset, and D. Helfritch. “Adiabatic Shear Instability Based Mechanism for
Particles/Substrate Bonding in the Cold-gas Dynamic-spray Process,” *Mater. Des.*, 2004, 25(8): 681.
- [7] Gyuyeol Bae Kicheol Kang Hyuntaek Jay-Jung Kim Changhee Lee, “Effect of particle size on the microstructure and
properties of kinetic sprayed nickel coatings,” *Surface & Coating Technology*, doi:10.1016/j.surfcoat.2010.03.046.
- [8] Peter C.King Saden H.Zahiri Mahnaz Jahedi, “Microstructural Refinement within a Cold-Sprayed Copper
Particle”. *Metallurgical and materials transactions A*. doi:10.1007/s11661-009-9882-5. June.2009.
- [9] *Abaqus Analysis User’s Manual*, Abaqus 6. 7 HTML Documentation, Dassault Systemes, 2007.
- [10] G. Eason, B. Noble, and I. N. Sneddon, “On certain integrals of Lipschitz-Hankel type involving products of Bessel
functions,” *Phil. Trans. Roy. Soc. London*, vol. A247, pp. 529–551, April 1955.